Simultaneous SHG of orthogonally polarized fundamentals in single QPM crystals

Benjamin F. Johnston*[a], Solomon M. Saltiel[b], Michael J. Withford[a] and Yuri S. Kivshar[c]
[a]Centre for Ultrahigh bandwidth Devices for Optical Systems and the Centre for Lasers and Applications, Macquarie University, Sydney, Australia, 2109.
[b]Faculty of Physics, University of Sofia, 5 J. Bourchier Boulevard, Sofia, BG-1164, Bulgaria
Nonlinear Physics Centre and Centre for Ultrahigh bandwidth Devices for Optical Systems
Research School of Physical Sciences and Engineering,
Australian National University, Canberra, ACT 0200, Australia
* benjamin@ics.mq.edu.au

ABSTRACT

Fabrication of quasi-phase-matching (QPM) gratings suitable for cascading of two second-order parametric nonlinear processes in a single lithium niobate crystal is being undertaken using a new technique - electric field poling assisted by laser micro-machined topographical electrodes. To date, single period poled gratings with 45.75, and 45.8 μm periods have been fabricated in order to demonstrate second harmonic generation of 1064nm laser light with 1st order type-I and 7th order type-0 QPM simultaneously. The two frequency doubling processes share a common Z polarized second-harmonic wave which allows exchange of energy between the two orthogonally polarized fundamental waves and several second order cascading interactions can be realized. The use of the higher QPM orders (3rd, 5th or7th) for the type-0 second harmonic generation process leads to comparable efficiencies of the two processes, as the respective nonlinear coefficients are $d_{zzz} \sim 27$ pm/V and $d_{yyz} \sim 4.7$ pm/V in lithium niobate crystals. Possible applications include; polarization switching, parametric amplification and polarization mode dispersion monitoring, and polarization insensitive second harmonic generation.

Keywords: Nonlinear optics, QPM, PPLN, laser micromachining

1. INTRODUCTION

Quasi-phase-matching materials are popular nonlinear optical media due to the versatility, efficiency and accompanying waveguide technologies they offer. QPM materials make use of a modulated second-order susceptibility to compensate for group velocity mismatch in second order nonlinear processes. Materials used for quasi-phase-matching include electric field poled lithium niobate, lithium tantalate and potassium titanyl phosphate as well as orientation patterned semiconductors. Some of the more recent innovations in the field include QPM gratings designed to phase-match several nonlinear processes in the same region of grating, allowing for multi-purpose crystals and cascading of nonlinear processes. In this manuscript we present the results of an investigation into simultaneous phase-matching of two SHG processes, involving the same wavelengths but with two orthogonally polarized fundamental components taking part. We will also briefly outline the laser fabrication technique we use for rapid prototyping of the periodically poled lithium niobate (PPLN) crystals used in these experiments. Potential applications for this simultaneously phase-matched, process, which include polarization independent SHG, SHG power control, polarization switching and elementary polarization mode dispersion (PMD) monitoring will be discussed.

2. SIMULTANEOUS TYPE-0 AND TYPE-I QPM IN LITHIUM NIOBATE

Electric field poled lithium niobate is perhaps the most popular QPM material because of its large nonlinear coefficients, wide availability as a low cost, high quality material, and well established waveguide technologies which make it suitable for integration into optical systems. Most QPM processes in lithium niobate are designed to target the largest nonlinear coefficient in lithium niobate, d_{33}. In terms of 3-wave mixing, we denote this as the "type-0", zzz - eee case, as the d_{33} coefficient couples z polarized pumps or fundamentals to z polarized harmonic, sum frequency, or parametric waves and the refractive indices these waves see are the extraordinary refractive indices as lithium niobate is a negative uniaxial crystal. Lithium niobate does however have an appreciable d_{31} coefficient which can be used for

QPM of "type-I" processes, which in lithium niobate are yyz – ooe processes, where y polarized pumps or fundamentals couple to z polarized harmonics, sum frequency, or parametric waves. Despite the lower efficiency of the type-I processes compared to 1st order type-0, they can still be an attractive alternative for processes in the visible region as the fabrication requirements for 1st order gratings, in terms of the period and domain size, are often easier to satisfy for type-I processes. Type-I processes in lithium niobate also have a broader wavelength acceptance range, allowing for implementation of nonlinear processes in broader bandwidth systems with lower power and bandwidth penalties [1]. Fig. 1 shows the required fabrication periods for type-0 and type-I QPM, as a function of crystal temperature, for SHG in PPLN for some common laser wavelengths of interest for visible light and C-band applications. The temperature dependant sellmeier relations for this and subsequent calculations have been taken from Dmitriev [2]. We have investigated the case where we employ a particular grating period which simultaneously phase-matches a 1st order type-I SHG or 7th order type-0 SHG. While using a 7th order grating is usually not desirable due to the greatly reduced efficiency, when comparing nonlinear coefficients we will be using in lithium niobate we find,

$$\frac{d_{33}}{7d_{31}} = \frac{27\,pmV^{-1}}{7 \times 4.7\,pmV^{-1}} 0 = 0.91 \tag{1}$$

so that the two QPM processes will in fact have very similar effective nonlinear coefficients in an ideal grating, which is a desired property the purpose of demonstrating polarization independent SHG by having both processes simultaneously phase-matched.
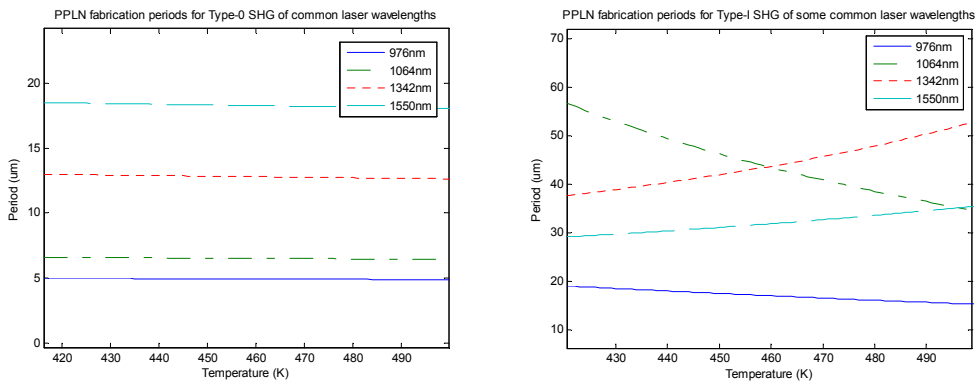

Fig. 1. PPLN fabrication periods for SHG of some common laser lines. Left: Required periods for 1st order type-0 (zzz) SHG. Right: required periods for 1st order type-I (yyz) SHG.

We have performed our simulations and experiments with the common Nd laser line 1064nm. Fig. 2 shows the required fabrication periods as a function of temperature for the 7th order type-0 and 1st order type-I processes at 1064nm. The intersection of these curves at a period of 45.76μm and a crystal temperature of 451K (178ºC) are our target fabrication period and operating temperature for achieving simultaneous phase-matching.
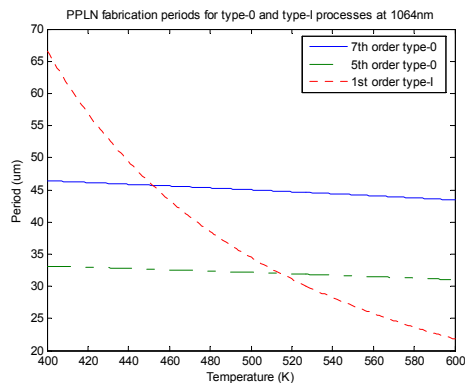
Fig. 2. Required fabrication periods for type-I and 5th and 7th order type-0 at 1064nm. The fabrication periods are coincident at 45.76μm for the 7th order type-0 and 32.2μm for the 5th order.

To consider the implications of having simultaneously phase-matched type-0 type-I SHG we will consider the coupled field equations (with slowly the varying amplitude approximation). The key feature of these equations is that the expression for the second harmonic contains contributions from both fundamentals, as the second harmonic field has a common polarization in both the type-0 and type-I processes.

$$\frac{dE_y^{\omega}}{dx} = -i\sigma_1 E_z^{2\omega} E_y^{\omega *} \exp\left(-i\Delta k_1 x\right) \tag{2}$$

$$\frac{dE_z^{\omega}}{dx} = -i\sigma_2 E_z^{2\omega} E_z^{\omega *} \exp\left(-i\Delta k_0 x\right) \tag{3}$$

$$\frac{dE_z^{2\omega}}{dx} = -i\sigma_3 E_y^{\omega} \exp\left(i\Delta k_1 x\right) - i\sigma_4 E_z^{\omega} \exp\left(i\Delta k_0 x\right) \tag{4}$$

Here the vectors E are the electric fields propagating in the x-direction whose superscript denote the optical frequency and the subscript denote the polarization with respect to the crystal axes. The parameters σ are given by:

$$\sigma_1 = \frac{2\pi d_{31}}{\lambda n_0} q_1, \quad \sigma_2 = \frac{2\pi d_{33}}{\lambda n_e} q_7, \quad \sigma_3 = \frac{2\pi d_{31}}{\lambda n_0} q_1, \text{ and } \sigma_4 = \frac{2\pi d_{33}}{\lambda n_e} q_7,$$

where $q_1 = 2/\pi$ and $q_7 = 2/7\pi$ are the QPM reduction factors for 1st and 7th order processes, n_o and n_e are the ordinary and extraordinary refractive indices of lithium niobate at the fundamental wavelength λ. Δk_0 and Δk_1 are the residual phase-mismatches in the system for the type-0 and type-I processes respectively, given as:

$$\Delta k_{0,1} = k_e^{2\omega} - 2k_{e,o}^{\omega} - G_{m=7,1} \tag{5}$$

Where $k_{o,e}^{\omega,2\omega} = \frac{n_{o,e}\omega,2\omega}{c} = \frac{2\pi n}{\lambda}$ are the wave-numbers for the participating fields. G_m is the contribution from the QPM structure, which for simple periodic domain structures is simply the inverse vector of the period Λ,

$$G_m = \frac{2\pi m}{\Lambda} \tag{7}$$

where m is the order of the QPM which for 50% duty cycle periodic domains is an odd integer. In our case we have m=7 for the 7th order type-0 process and m=1 for the 1st order type-I process. The ideal case is to have both processes simultaneously phase matched so that $\Delta k_0 = \Delta k_1 = 0$, which can be achieved with careful design and fabrication of the QPM structure. We can gain incite into the behavior of the simultaneously phase-matched system by considering the case of negligible depletion of the fundamental components. Integrating equation 4 over a crystal length L and assuming steady fundamental fields.

$$E_z^{2\omega} = \int_0^L \frac{dE_z^{2\omega}}{dx} = -\sigma_3 E_y^{\omega 2} L \exp(i\Delta k_1 L/2) sinc(\Delta k_1 L/2) - \sigma_4 E_z^{\omega 2} L \exp(i\Delta k_0 L/2) sinc(\Delta k_0 L/2) \tag{8}$$

We must keep in mind that the two fundamental fields may not necessarily have the same phase or amplitude. As such we introduce them as basic plane waves in the following manner;

$$E_y^{\omega 2} = A_y^2 \exp\left(2i\omega t\right)$$
$$E_z^{\omega 2} = A_z^2 \exp\left(2i\omega t + 2i\phi\right) \tag{9}$$

Where A_y and A_z are the field amplitudes, and ϕ is the net phase difference between the two fields.

At ideal phase-matching conditions all the terms containing Δk are unitary and the irradiance of the SH can be found as,

$$E_z^{2\omega} = -\sigma_3 A_y^2 e^{2i\omega t} L - \sigma_4 A_z^2 e^{2i(\omega t + \phi)} L$$
$$I^{2\omega} = E * E = \sigma_3^2 A_y^4 L^2 + \sigma_4^2 A_z^4 L^2 + 2\sigma_3\sigma_4 A_y^2 A_z^2 \cos(2\phi) \tag{10}$$

We can see from equation 10 that the SH irradiance at phase-matching will depend quadratically on the irradiance of the fundamentals but also the relative phase ϕ between them. In fact, if we have anti-phase fundamentals, $\phi = \pi/2$, with equal contributions to Eq 10 such that $\sigma_3^2 A_y^4 = \sigma_4^2 A_z^4$ then we see,

$$I^{2\omega} = \sigma_3^2 A_y^4 L^2 + \sigma_4^2 A_z^4 L^2 - 2\sigma_3\sigma_4 A_y^2 A_z^2 = 0 \tag{11}$$

and the SH output is suppressed completely. Arbitrary input amplitudes and phases can regulate the SH output anywhere between zero and its peak efficiency. In practice the fundamental input states can be prepared by wave-plates and/or electro-optic means.

3. LASER ASSISTED FABRICATION OF POLED LITHIUM NIOBATE

We use a novel approach for fabricating our PPLN using laser micromachining methods, as first reported by Reich *et al* [3], and which we have investigated the associated domain kinetics [4]. While the now conventional method of electric field poling the crystal in a liquid electrolyte [5] is used, the electrode structure on the crystal surface is fabricated by laser machining into the crystal surface rather than using lithographically defined conductive electrodes as are commonly used. The topographical structure which is laser machined into the crystal surface produces strong anisotropy in the electric field when poling in an electrolyte solution. Fig. 3 shows the potentials and electric field strength for a v-groove geometry when poled in an electrolyte cell. Experimentally we see strong evidence of the predicted field distribution at work, as shown in fig. 4. Domains tend to nucleate and grow from a single region at the apex of the scribe where the field gradient is the highest. We also see regions of unreversed crystal adjacent to the scribe, due to the reduced field gradient at the shoulders of the scribe as predicted in the simulations.
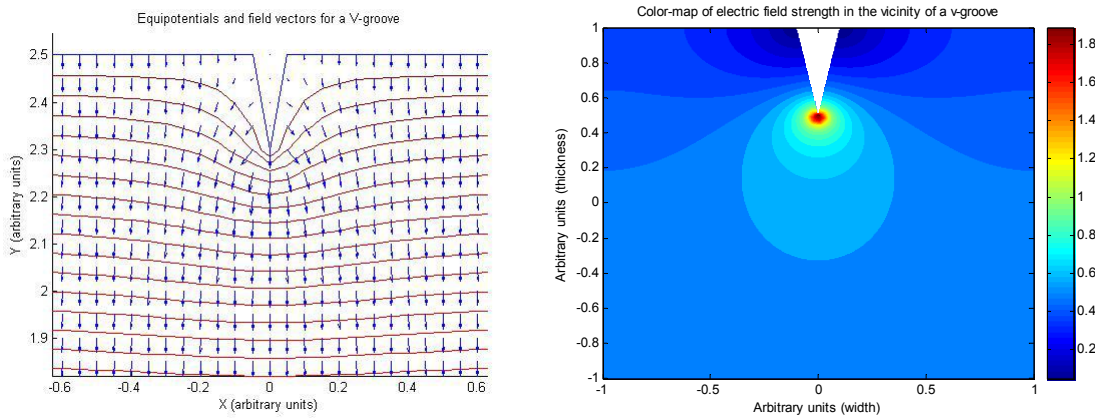

Fig. 3. Electrostatic simulations of a V-groove geometry similar to that produced by laser machining. Left: equipotential lines and corresponding electric field vectors. Right: colormap plot of electric field strength in the vicinity of the V-groove.
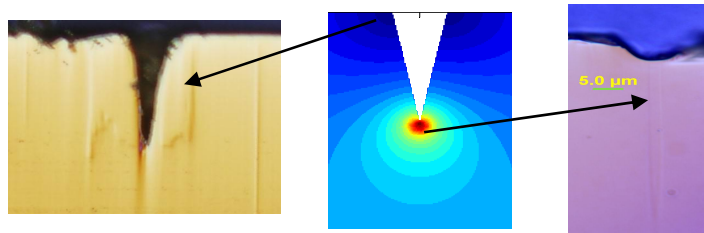

Fig. 4. Evidence of the electric field distribution from poled samples. Left: regions of unreversed crystal adjacent to the V-groove due to the reduced electric field at the groove shoulders. Right: single regions of domain nucleation and propagation originating from the high electric field produced at the apex of the V-groove.

While this technique may not be well suited to wafer scale fabrication, it has proven to be very useful for fabricating experimental samples with various periods and patterns in quick time, and without the expense of designing and fabricating lithographic masks and using clean room facilities. Good quality PPLN with periods down to 20μm can be achieved in 500μm thick crystal. Below this period reliable domain formation can be problematic, and an investigation on the limitations and possible improvements of this technique is underway. The technique is very well suited to our target application where we are using periods in excess of 30μm. The periodicity of our gratings can be controlled by translation stages to resolutions of 50nm.

The laser system used for the electrode fabrication was a Spectra-Physics Hurricane, with a 1kHz pulse train and 120fs pulses at a central wavelength of 800nm. The pulses were focused onto the sample using a 10x objective lens, and sample translation was carried out using a set of XYZ Aerotech ATA stages. Pulse energies of 3μJ were used and could be focused into a sub 5μm spot, producing fluences of ~4Jcm^{-2}. This regime was found to provide sufficient material removal without causing significant fracturing of the surrounding crystal.

Inspection of the crystal domain structure was carried out using simple polishing and phase-contrast microscopy rather than the conventional acid etching. It was found that domains in lithium niobate will polish differentially using wet AlO$_2$ polishing, but with much less physical contrast than that observed by acid etching. The lack of physical contrast is easily overcome by viewing the polished surface under phase-contrast microscopy. Domain etchings produced by polishing can be little as 100nm for 10min polishing time, but these small reliefs are easily viewed as significant path differences under phase-contrast microscopy.
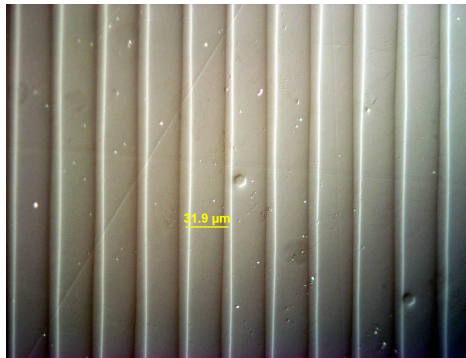

Fig. 5 Domains in lithium niobate revealed by conventional polishing and viewed under phase-contrast microscopy.

4. EXPERIMENTAL SETUP AND RESULTS

The PPLN crystal which was used in these experiments was fabricated with two gratings, 45.75μm and 45.8μm, which were within the 50nm stage resolution of the target period, 45.766μm. A microscope image of one of these gratings is shown in fig. 6. The gratings consisted of 100 periods, 4.6mm long, and upon poling an average duty cycle of ~35% was produced. The end faces of the crystal were polished but left uncoated.
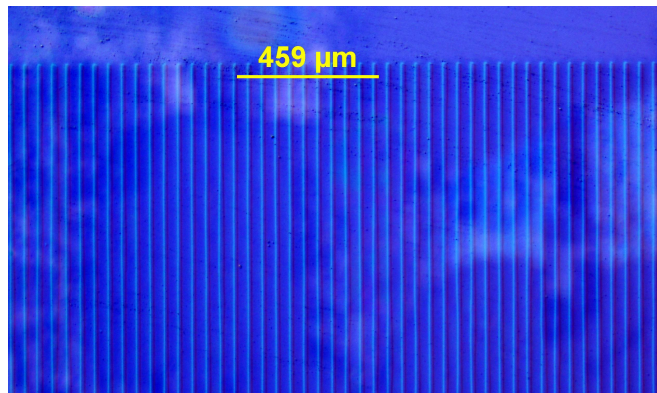

Fig. 6. A section of one of the gratings used for the optical experiments. The crystal was 4.6mm long, containing 100 domains.

The setup for the second harmonic experiments is shown in fig. 7. The laser used was an in-house built Nd:YVO$_4$ laser running on the 1064.5nm line. The laser was Q-switched at 10Hz, producing 20ns pulses. The laser had an average power of 300mW, and an estimated pulse peak power of 3kW. The PPLN crystal was housed in an oven controlled by a Eurotherm microcontroller. The laser was focused into the crystal by a 50mm IR lens. The polarization to the crystal

was controlled using a half-wave-plate (HWP) and a quarter-wave-plate (QWP) was used in tandem for measurements where a π/2 phase difference has been applied between the input polarization components. A Glan prism was used to resolve the polarizations at the output and average power detectors were used to monitor power on either arm of the Glan. Any SH produced was always vertically polarized and was measured on the side arm of the Glan prism. The first measurements made were the temperature acceptance curves for the type-0 and type-I SHG. These measurements were performed by setting the HWP to the appropriate input polarization and recording the SH as the crystal temperature was dropped through phase-matching. The results for the two gratings are shown in fig 8.
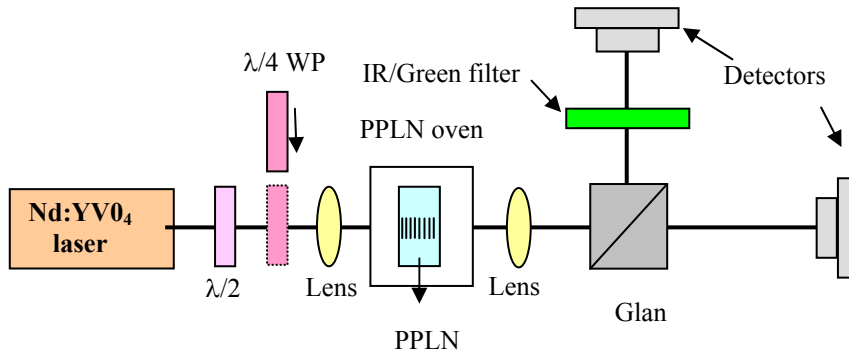

Fig. 7. Experimental layout for SHG from two simultaneously phase-matched processes.

While both gratings exhibited some overlap of the phase-matching curves, the 45.8μm grating showed good overlap of the phase-matching peaks for both processes. The fact we see such good overlap at 45.8μm, rather than the predicted period of 45.76μm, suggests that the actual sellmeier relations for the crystals we have used differ from reference. The departure from the ideal sinc^2 curves for the 7th order processes is due to the higher order processes being extremely sensitive to duty cycle and periodicity fluctuations in the crystal domain structure. We also see that the sensitivity to fabrication errors for the 7th order processes means lower than ideal efficiencies. We see the 7th order processes exhibiting at best 50% of the efficiency of the 1st order curves, rather than the 80% predicted from the squaring of equation 1.
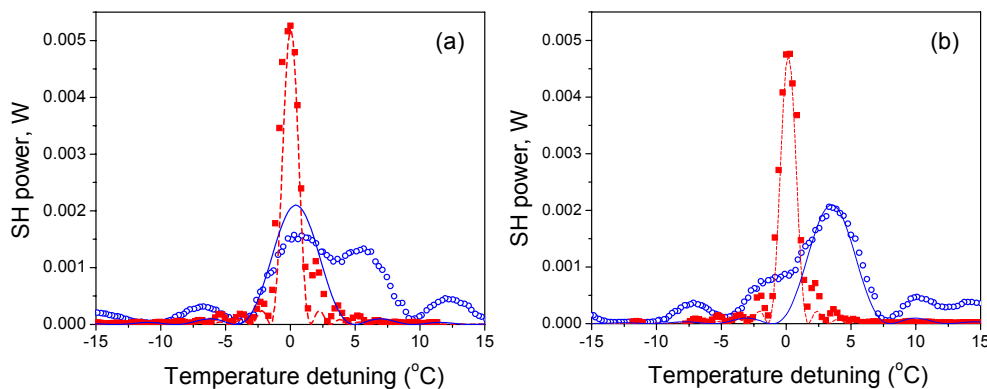

Fig. 8. Temperature acceptance curves for QPM SHG at 1064nm with type-I and 7th order type-0 phase-matchings. a) PPLN with fabricated period of 45.8μm. b) PPLN fabricated with 45.75μm period.

The effect of the input polarization on the SHG output was investigated by using wave-plates to prepare the laser polarization. The effect of varying the direction of the linear polarization was measured by rotation of the HWP, shown as the blue/open markers and curve in fig. 9. The maximum value of the SH is indicative of the type-I process and the

minimum value indicative of the type-0, with some amount of SH being produced for all linear input polarizations. A QWP was then introduced with its fast axis aligned to the z-axis of the lithium niobate crystal. The HWP was then rotated as before, producing elliptically polarizations such that the z and y fundamental components were always launched with a π/2 phase difference. The resulting effect on the SH power is shown as the red/solid markers and curve in fig. 9. With the π/2 phase difference we see that the SH goes to zero at a particular HWP setting, due to the competing anti-phase fundamental components as described by Eq (11). The SH level for the linear input polarizations, where the HWP has been aligned with a crystal and QWP axis, are the same as for the case without the QWP, as expected.
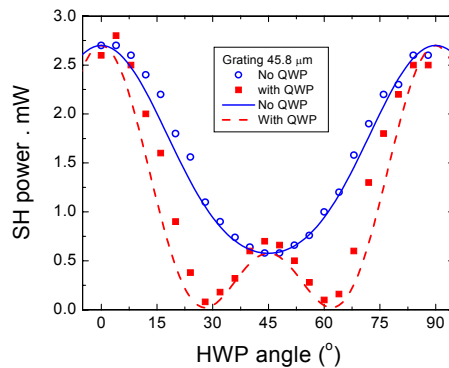

Fig. 9. SH at phase-matching as a function of the input polarization. The blue curve/markers indicate the SH as a function of the linear input polarization, as indicated by rotation of a HWP. The red curve/markers indicate the SH as a function of elliptically polarized input when using a QWP in tandem with the rotating HWP.

The temperature dependence on the process was also measured, with the HWP set to where the SH zero was observed and the crystal temperature being dropped through phase-matching with the SH being recorded. This was conducted for both the case of the QWP in and out of the setup. The results are shown in fig. 10. For the case of no QWP we see a constructive combination of the curves of the two individual temperature acceptance curves shown in fig. 8. When the QWP is introduced we see destructive combination of the curves, including the secondary $sinc^2$ lobes from the type-I process combining with the broadened primary lobe of the type-0 process.
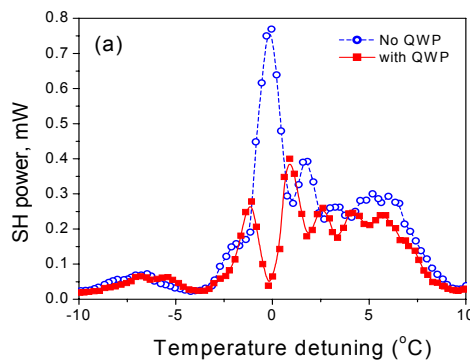

Fig. 10. SHG temperature acceptance curves when both fundamental components are launched. Blue/open markers and curve show the case for linear polarization, showing constructive combination of SH. Red/solid markers and curve indicates the case for elliptically polarized input, prepared with an additional QWP, showing destructive combination of the SH.

The effect of an arbitrary phase-difference between the fundamental components has also been investigating by using a variable retardence plate in place of the QWP. This was implemented using a Berek polarization controller from Newfocus which includes a variable retardence plate, where the retardence is controlled by the tilt angle of a

birefringent plate. An initial linear polarization was set at 45º so that both processes had contributions from their fundamental components. The Berek was then used to set an arbitrary retardence between the two polarizations. The measurement of SH power as a function or retardence is shown in fig 11. We see that the SH level falls as the retardence is increased, to a minimum level when we have a ¼ wave ($\pi/2$) retardence and anti-phase fundamentals, and then returns to the initial level as we approach ½ wave (π) retardence.
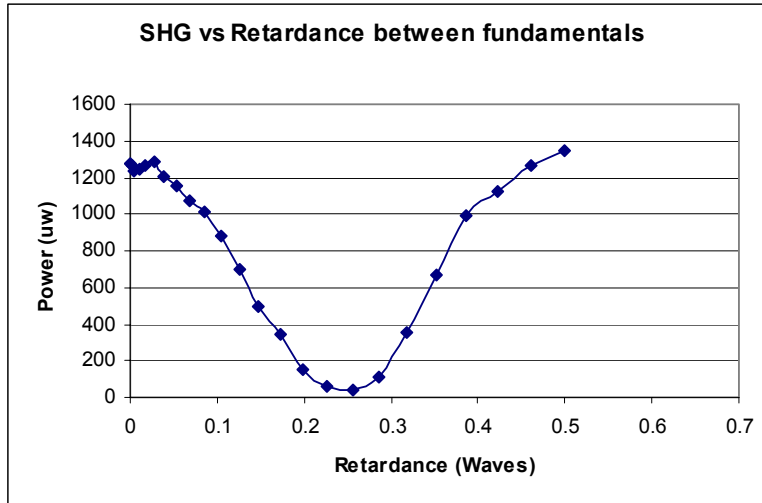

SHG vs Retardance between fundamentals

Fig 11. SH power as a function of the retardence between two similar fundamental components which are simultaneously phase-matched in a PPLN crystal.

5. DISCUSSION

There are a number of potential applications which may utilize the simultaneously phase-matching we have described here. The most straight forward application is a device which regulates the level of SH coming from a visible system by controlling the phase between the fundamental's polarization components. This could be achieved using an electrooptic phase controller and power feedback to stabilize the level of SH produced by the PPLN crystal. A conceptual diagram of the device is shown in fig 12. Such a system may be useful in applications requiring stabilization and control of visible laser power levels such as pumping Ti:Sapph oscillators and laser display applications.
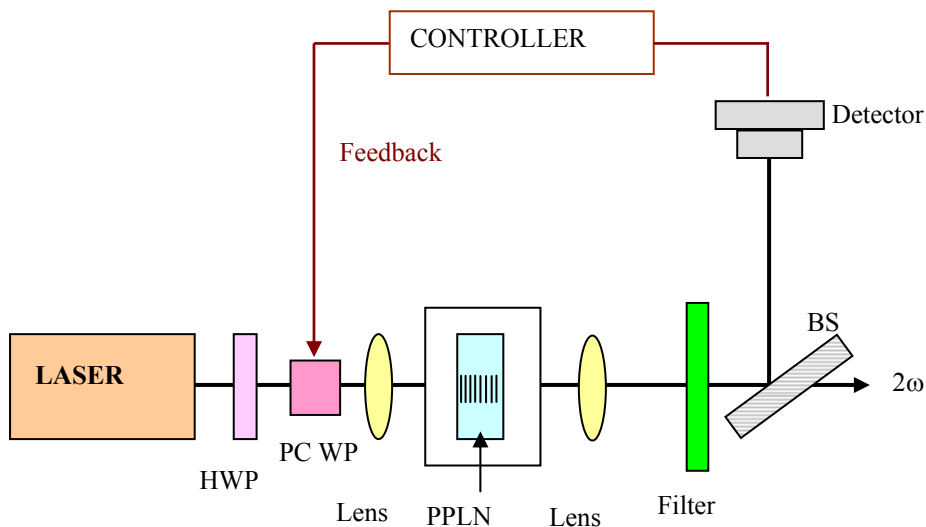

Fig 12. Schematic of a conceptual system based on simultaneously phase-matched SHG, which regulates the level of SH power being produced by electro-optically controlling the input polarization of the fundamental.

Another potential application is the monitoring of low order polarization mode dispersion (PMD). PMD is one of the problems which contribute to the limitation and degradation of high speed optical links. PMD is caused by fabrication imperfections or environmental variations in and around the waveguides or optical fibers making up the optical link. These factors can cause refractive index perturbations in the guiding material, resulting in some average birefringence over the flight-time through the guide. This leads to some polarization components of the optical signal traveling at different velocities relative to the average, temporally broadening the optical pulses carrying the data. This can limit the distance, bit-rate and pulse duty-cycle that can be utilized by the optical link, as pulses can be broadened to the extent of becoming indistinguishable.

Since the simultaneously phase-matched SHG we have demonstrated here depends both on the relative phase and amplitudes of the fundamental polarization components, we have the makings of a 1st order PMD monitor. Once the relative nonlinearities of the two SHG processes have been determined (as fig. 9 shows), an arbitrary input polarization state, coming from a waveguide or fiber and whose orientation to the crystal could be controlled by a HWP, can be determined based on the level of SH being produced in the crystal. In a simple control system where monitoring the retardance between orthogonal polarizations is of interest, a curve similar to fig. 11 could be used as calibration for using the SH as a monitor.

Other opportunities for this type of phase-matching include polarization switching via seeded, degenerate, parametric down conversion (backwards harmonic generation). This processes requires efficient SHG from one of the input polarizations and then seeding from the other polarization to convert the SH back into the fundamental wavelength, but at the orthogonal polarization of the seeding fundamental. This process can be simulated by integrating the couple equations (1-3) with the appropriate initial conditions, but requires higher than practical peak powers to achieve complete polarization switching, as shown in fig. 13, however low levels of polarization switched degenerate parametric amplification may still be suited for some applications, including the regeneration and amplification of optical signals. Simultaneous phase-matching may also be applicable to applications utilizing spontaneous parametric down conversion, as there will be a probability of producing a down converted photon pair of either polarization when both type-0 and type-I processes are phase-matched.
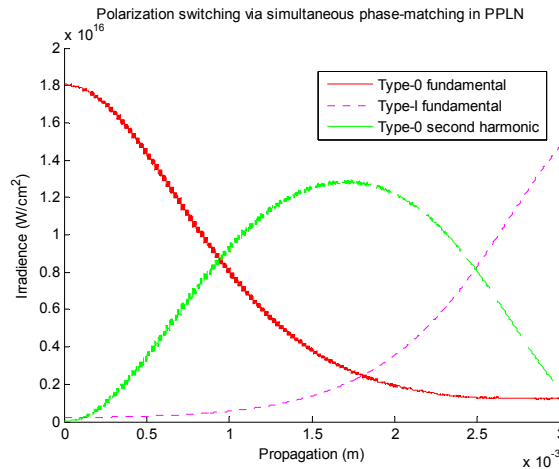

Fig 13. Simulation of polarization switching of the fundamental wavelength via efficient SHG cascaded with seeded parametric down conversion (backward harmonic generation).

PPLN fabrication periods of interest other than those used here include 36.17μm for simultaneous phase-matching of 3rd order type-0 and 1st order type-I SHG in the m-band around 1.3μm at 371K (98.7C), or alternatively 58.29μm for the 5th and 1st order case at 482K (209C). Also, due to the fortunate dispersion and birefringent properties of lithium niobate, two useful type-I SHG processes at 1064nm and 1342nm can be phase-matched simultaneously with a period of 43.58μm at 459K (186C). This particular case may be especially useful for red/green dual wavelength Nd lasers

running on both these fundamental lines. Such a system could operate the fundamental lines either simultaneously or alternatively, by adjustment of a cavity optical element such as the output coupler, and the nonlinear crystal would not need tuning or changing.

Operation in the C-band will require a more complicated grating structure such as a phase-reversed or aperiodic grating. However, if the correct duty cycle for a 2nd order type-0 process can be fabricated there is the opportunity to use a 36μm period grating at 504K (230C) to achieve simultaneous phase-matching of 2nd order type-0 and 1st order type-I SHG.

6. CONCLUSION

We have demonstrated simultaneous phase-matching of two SHG processes, 7th order type-0 and 1st order type-I, in single period PPLN, by careful selection of the grating period. The PPLN crystals described here have been fabricated using a rapid prototyping technique based on laser micromachining. Simultaneously phase-matching these two processes leads to internal interference of the fundamentals and regulates the amount of SH that is produced when components of both fundamental polarizations are present. Conversely the, SH power may be used as an indication of the fundamentals input polarization state. Suggested applications for such crystals include SH power regulation, polarization independent SHG for randomly polarized sources such as fiber lasers, low order polarization mode dispersion monitoring in optical waveguides and parametric down conversion processes.

REFERENCES

1. Y. Chen, R. Wu, X. Zeng, Y. Xia, and X. Chen, "Type I quasi-phase-matched blue second-harmonic generation with different polarizations in periodically poled LiNbO$_3$," Opt. Laser Technol. **38**, 19–22 (2006).
2. G. G. Gurzadian, V. G. Dmitriev, and D. N. Nikogosian, "Handbook of Nonlinear Optical Crystals," 3rd ed., Vol. 64 of Springer Series in Optical Sciences (Springer-Verlag, New York, 1999).
3. M. Reich, F. Korte, C. Fallnich, H. Welling, and A. Tunnermann, "Electrode geometries for periodic poling of ferroelectric materials," Opt. Lett. **23**, 1817-1819 (1998).
4. B.F. Johnston and M.J. Withford, "Dynamics of domain inversion in LiNbO$_3$ poled using topographic electrode geometries", Appl. Phys. Lett. **86**, 262901 (2005).
5. L. E. Myers, R. C. Eckardt, M. M. Fejer et al., "Quasi-phase-matched optical parametric oscillators in bulk periodically poled LiNbO$_3$," J Opt Soc Am B **12** (11), 2102-2116 (1995).